Chinese Medicine

RESEARCH

Integrated quality evaluation strategy for multi-species resourced herb medicine of Qinjiao by metabolomics analysis and genetic comparation

Zeyun Li[1] , Yue Du[1], Yongliang Yuan[1], Xiaojian Zhang[1], Zhengtao Wang[2*] and Xin Tian[1*]

Abstract

Background: Quality evaluation of multi-species resourced herb medicine (MSRHM) is a main problem for quality control of herb medicine. Current quality evaluation methodology lost consideration of species discrepancy. New quality evaluation strategy for MSRHM is in urgent need. Qinjiao, a representative MSRHM, originated from *Gentiana macrophylla* Pall., *Gentiana straminea* Maxim., *Gentiana crassicaulis* Duthie ex Burk. or *Gentiana dahurica* Fisch., has been used as an important herb medicine over 2000 years for expelling wind-dampness and relieving impediment pain. However, quality evaluation among species has never been revealed. The current work proposes an integrated quality evaluation strategy for MSRHM of Qinjiao, which may promote innovation of quality control of MSRHM.

Methods: In this work, 58 batches of Qinjiao covering 4 species were collected. Genetic comparative analysis based on ITS2 sequence was conducted. Metabolomics analysis based on TOF–MS and NMR spectrum were carried out. Compounds underlying species differences were identified and their discrepancies among species were investigated by ANOVA analysis and multivariate analysis.

Results: Four species of Qinjiao can be authenticated by ITS2 sequence comparation. Metabolomics analysis by TOF/MS and NMR revealed chemical discrepancies among species of Qinjiao. Maximum discrepancy was present between *Gentiana crassicaulis* Duthie ex Burk. and *Gentiana dahurica* Fisch. Chemical difference among species were tentative explored. For TOF–MS profiling, 28 constituents were tentative identified, 17 of which were further confirmed by standards. For ^{1}H-NMR profiling, signals from 5 compounds were assigned. Contents discrepancies were investigated by ANOVA analysis. It seems that (seco)iridoids like loganic acid, gentiopicroside or swertiamarin were richer in specie of *Gentiana crassicaulis* Duthie ex Burk., while flavonoid (morroniside) and triterpenoids (roburic aicd, ursolic acid, oleanolic acid, β-sitosterone) were richer in specie of *Gentiana dahurica* Fisch. The current research demonstrates that metabolite profiling based on both UPLC/Q-TOF MS and ^{1}H-NMR coupled with ITS2 sequence comparation can be a powerful tool for quality investigation of MSRHM of Qinjiao.

Conclusions: A comprehensive quality evaluation strategy for MSRHM was proposed by integrating UPLC-Q-TOF–MS, NMR based metabolic analysis and ITS2 sequence genetic comparation. The proposed quality evaluation strategy shall promote innovation of quality control of traditional Chinese medicine.

Keywords: Quality evaluation, Multi-species resourced herb medicine (MSRHM), Qinjiao, ITS2, Metabolomics

---

*Correspondence: ztwang@shutcm.edu.cn; tianx@zzu.edu.cn
[1] Department of Pharmacy, The First Affiliated Hospital of Zhengzhou University, Zhengzhou 450052, China
[2] Institute of Chinese Materia Medica, Shanghai University of Traditional Chinese Medicine, Shanghai 201203, China

Li *et al. Chin Med*   (2020) 15:16

Page 2 of 14

Background

Quality control of multi-species resourced herb medicine (MSRHM) is a main problem for quality control of herb medicine. Current quality control methodology bears disadvantages of lacking consideration of species discrepancy, ignoring the fact that discrepancies among species were inevitable and shall produce different chemical component and clinical effects. As a result, new quality investigation strategy for MSRHM is in urgent need.

Qinjiao, namely *Gentianae Macrophyllae* Radix, is an ancient Chinese herb medicine and has been described and recorded in several ancient Chinese Medicine monographs like Shen Nong's Herbal Classic (Han Dynasty, Shen Nong Ben Cao Jing), Compendium of Materia Medica (Ming Dynasty, Ben Cao Gang Mu) [1] and also in Chinese pharmacopoeia. Over 2000 years, Qinjiao has been utilized to treat a wide range of diseases, including hypertension, osteoarthritis, and especially rheumatism [2]. According to China Pharmacopoeia 2015 version [3], Qinjiao consists of the dried roots of *Gentiana macrophylla* Pall. (*G. macrophylla*), *Gentiana straminea* Maxim. (*G. straminea*), *Gentiana crassicaulis* Duthie ex Burk. (*G. crasicaulis*) or *Gentiana dahurica* Fisch. (*G. daurica*). As a represented MSRHM, quality and efficacy of Qinjiao among species were inevitable variable [4, 5]. Former researches mainly focused on contents determination or chemical profiling of certain kind of Qinjiao [6, 7], or even chemical and genetic analysis of *G. crasicaulis* and *G. macrophylla* [8]. No systematic species investigation for four kinds of Qinjiao has been revealed, which may shed new light into quality control and clinical utilization of Qinjiao.

DNA barcode of internal transcribed spacer 2 (ITS2) is prevalently adopted as a universal barcode for plant, especially herbal medicinal identification [9]. ITS2 barcode has been successfully employed for species identification of Qinjiao [8, 10]. Chemical profiling combined with multivariate analysis provided systematic chemical comparison of metabolites, and can be powerful tool for species investigation of MSRHM [11]. Ultra-performance liquid chromatography quadrupole time-of-flight mass spectrometry (UPLC-Q-TOF–MS) and proton nuclear magnetic resonance spectrometer (^{1}H-NMR) are the most frequently employed platform for metabolic profiling.

Herein, this research collected 58 batches of Qinjiao, covering four species, originated from main producing areas of China (Gansu, Shanxi, Hebei, Shaanxi, Heilongjiang, Liaoning, Nei Mongol, Yunnan, Szuchuan, Qinghai, Tibet). Genetic comparative and metabolic profiling analysis of four species of Qinjiao were carried out. First, all herbs were authenticated by morphological identification as well as DNA barcoding comparison. Then, chemical profiles were acquired by UPLC-Q-TOF–MS and ^{1}H-NMR. Third, metabolomics based species investigation, including principal component analysis (PCA) and orthogonal partial least squares discrimination analysis (OPLS-DA), was conducted to reveal the quality discrepancy among species. Finally, an integrated quality evaluation strategy for MSRHM of Qinjiao by UPLC-Q-TOF–MS, NMR based metabolomics analysis and ITS2 sequence genetic comparation was established. The flow chart of the proposed methodology is shown in Fig. 1. The current work may facilitate quality control, utilization and species discrimination of different kinds of Qinjiao.

Materials and methods

Sample collection and preparation

Fifty-eight batches of rhizomes of *G. macrophylla*, *G. straminea*, *G. crasicaulis* and *G. daurica* were collected from different herbal markets or harvested from various locations of China. All samples were authenticated by Professor Jiuzhi Yuan (Shenyang Pharmaceutical

Fig. 1 The flow chart of the proposed methodology

Li *et al. Chin Med*   (2020) 15:16

Page 3 of 14
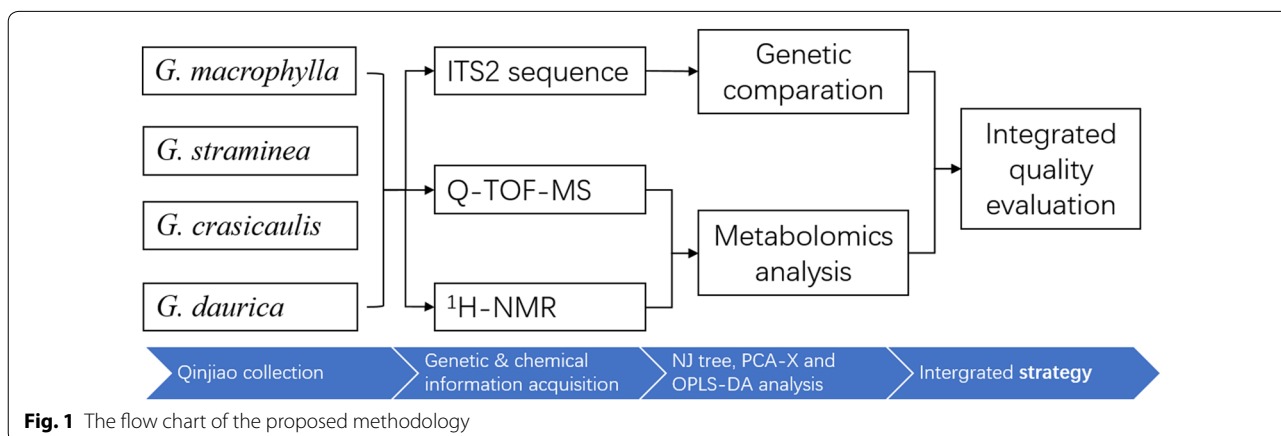
University) or Professor Lihong Wu (Shanghai University of Traditional Chinese Medicine). Voucher specimens were deposited in Department of Pharmacy, The First Affiliated Hospital of Zhengzhou University, Zhengzhou, China or the Institute of Chinese Materia Medica, Shanghai University of Traditional Chinese Medicine, Shanghai, China. Detailed information of collected samples in this study is list in Table 1. The roots were gently washed and dried at 50 °C for 48 h, and then were grounded into powder and stored in glass jars in the dark at room temperature until further analysis.

Chemicals and reagents
Methanol-d4 (CD3OD, 99.8%) was obtained from Cambridge Isotope Laboratories (Miami, FL, USA). Methanol of HPLC grade was purchased from Honeywell Inc. (Morristown, NJ, USA). Formic acid of LC–MS grade was bought from ROE Scientific Inc. (Newark, DE, USA). Deionized water was purified using a Milli-Q system (Millipore, Bedford, MA, USA). The chemical reference standards (CRS) of gentiopicroside, loganic acid, swertiamarin, sweroside, 6′-*O*-β-D-Glucosylgentiopicroside, roburic acid, morroniside, isovitexin, homoorientin, oleanolic acid, ursolic acid, β-sitosterone, citric acid, quercetin, kaempferol, and daucosterol were purchased from Chengdu Must Bio-techenology Co., Ltd. (Chengdu, China), with HPLC purity > 98%. All other chemicals and reagents were of analytical grade and commercially available.

Genetic Analysis of collected Qinjiao samples
ITS2 was prevalently adopted as a universal barcode for plant, especially herbal medicinal identification [9]. ITS2 barcode has been successfully employed for species identification of Qinjiao [8, 10]. In current research, ITS2 region was compared to verify the authentication of collected Qinjiao samples. To extract total genomic DNA from dried rhizomes (50 mg), the protocol provided by the Plant Genomic DNA Kit (Tiangen Biotech, Co., Ltd., Beijing, China) was used. Extracted DNA sample was stored at − 20 °C until use. The ITS2 sequence was amplified using a pair of primers (ITS2F: 5′-ATGCGA TACTTGGTGTGAAT-3′; ITS3R: 5′-GACGCTTCTCCA GACTACAAT-3′) described previously by Chen et al. [12]. The PCR amplification was conducted as described by Luo et al. [13]. Amplification products were examined by electrophoresis in 1% (wt/vol.) agarose gels and visualized under ultraviolet light to detect successfully amplified products and the possible contamination of negative controls. After purifying, the PCR products were directly subjected to sequencing.

Sequences were edited and assembled using DNAMAN software (version 6.0) and refined manually. ITS2

resuquence were identified using DNA barcoding system for identifying herbal medicine (http://www.tcmbarcode.cn). Genetic distances were calculated using the Kimura-2-Parameter (K2P) model. All the newly obtained ITS2 sequences were uploaded to GenBank.

UPLC-Q-TOF–MS profiles analysis of the collected Qinjiao
0.5 g power (through No. 3 sieve) of each Qinjiao sample was placed into a separate 50 mL stopper conical flask followed by the addition of 20 mL methanol. The mixtures were vortexed for 1 min, sonicated (40 kHz, 500 W) for 30 min. Cooling down to ambient temperature, the lost weight was made up by methanol. After centrifugation at 10,000 rpm, 4 °C for 10 min, a 2 μL aliquot of the supernatants was injected into a UPLC-ESI-Q-TOF system (AB Sciex, Framinghan, MA, USA) for MS analysis.

Chromatography separation was achieved on an ACQUITY UPLC HSS T3 column (100 × 2.1 mm i.d., 1.8 μm) maintained at 40 °C. The mobile phase consisted of A (0.1% formic acid in water) and B (0.1% formic acid in methanol), using gradient elution: 0–1 min, 5–30% B; 1–5 min, 30–40% B; 5–6 min, 40–90% B; 6–13 min, 90–100% B; 13–21 min, 100% B; 21.01–24 min, 5% B. The flow rate was set at 0.3 mL/min and the injection volume was 2 μL.

The mass spectrometric data were collected on a SCIEX X500R QTOF mass spectrometer (AB Sciex, Framinghan, MA, USA) coupled with an electrospray ionization interface in negative ion modes (ESI-). SCIEX OS software 1.2 (AB, Milford, MA) was employed for data acquisition and procession. The following parameters settings were used: the ion spray voltage of 4000 V; turbo spray temperature (TEM) of 600 °C; declustering potential (DP) of − 80 V; collision energy (CE) of − 45 V; nebulizer gas (gas 1) of 55 psi; heater gas (gas 2) of 55 psi, CAD gas of 7 psi, and curtain gas of 35. Nitrogen was kept as the nebulizer and auxiliary gas. TOF MS and TOF MS/MS were scanned with the mass range of *m/z* 50–1000. Continuous recalibration was carried out every six samples. In addition, dynamic background subtraction (DBS) trigger information-dependent acquisition (IDA) was used to trigger acquisition of MS/MS information of low-level constituents. The accurate mass and composition for the precursor ions and fragment ions were analyzed using the Markerview™ software (Version 4.1, Waters Co., Milford, MA, USA) integrated with the instrument.

QC samples were prepared by combining equal aliquots from all Qinjiao samples and were injected every six specimens during the whole analysis. QC data obtained was used to assess the stability of the LC/MS platform. For all QCs, 5 characteristic features (list in Additional file 1: Table S1) were picked out to verify the

Li *et al. Chin Med*   (2020) 15:16

Page 4 of 14

Table 1 Samples information of Qinjiao for metabolomics and ITS2 barcode analysis

Sample ID	Origins	Species	GenBank accession nos.
QJ01	Mongolian autonomous county of Henan, Tibetan autonomous prefecture of Huangnan, Qinghai province	*G. macrophylla* Pall.	MH602351
QJ02	Gonjo county, Qamdo city, Tibet	*G. crassicaulis* Duthie ex Burk.	MH602352
QJ03	Tibetan Qiang autonomous prefecture of Ngawau, Sichuan	*G. crassicaulis* Duthie ex Burk.	MH602353
QJ04	Nyingchi city, Tibet autonomous region	*G. crassicaulis* Duthie ex Burk.	MH602354
QJ05	Ganzi Tibetan autonomous prefecture, Sichuan province	*G. crassicaulis* Duthie ex Burk.	MH602355
QJ06	Maqu country, Gannan Tibetan autonomous prefecture, Gansua province	*G. straminea* Maxim.	MH602389
QJ07	Tibetan autonomous prefecture of Golog, Qinghai province	*G. straminea* Maxim.	MH602390
QJ08	Mongolian autonomous county of Henan, Tibetan autonomous prefecture of Huangnan, Qinghai province	*G. straminea* Maxim.	MH602391
QJ09	Ebian Yi Nationality autonomous county, Minle city, Sichuan province	*G. crassicaulis* Duthie ex Burk.	MH602356
QJ10	Hohhot city, Inner Mongolia	*G. straminea* Maxim.	MH602392
QJ11	Daguan country, Zhaotong city, Yunnan province	*G. crassicaulis* Duthie ex Burk.	MH602357
QJ13	Yulong naxi autonomous prefecture, Lijiang city, Yunan province	*G. crassicaulis* Duthie ex Burk.	MH602358
QJ14	Minle country, Zhangye city, Gansu provinice	*G. straminea* Maxim.	MH602393
QJ15	Xinzhou city, Shanxi province	*G. crassicaulis* Duthie ex Burk.	MH602359
QJ16	Gonghe town, Qingyang city, Gansu province	*G. macrophylla* Pall.	MH602387
QJ17	Barkam city, Tibetan Qiang autonomous prefecture of Ngawau, Sichuan	*G. crassicaulis* Duthie ex Burk.	MH602360
QJ18	Barkam city, Tibetan Qiang autonomous prefecture of Ngawau, Sichuan	*G. crassicaulis* Duthie ex Burk.	MH602361
QJ19	Barkam city, Tibetan Qiang autonomous prefecture of Ngawau, Sichuan	*G. crassicaulis* Duthie ex Burk.	MH602362
QJ20	Ruoergai County, Tibetan Qiang Autonomous Prefecture of Ngawau, Sichuan	*G. straminea* Maxim.	MH602394
QJ21	Ruoergai county, Tibetan Qiang autonomous prefecture of Ngawau, Sichuan	*G. straminea* Maxim.	MH602395
QJ22	Huating country, Pinliang city, Gansu province	*G. macrophylla* Pall.	MH602388
QJ23	Tongguan country, Weinan city, Shanxi province	*G. crassicaulis* Duthie ex Burk.	MH602363
QJ24	Malong country, Qujing city, Yunana province	*G. crassicaulis* Duthie ex Burk.	MH602364
QJ25	Huichuan town, Weiyuan country, Dingxi city, Gansu province	*G. crassicaulis* Duthie ex Burk.	MH602365
QJ26	Ludian country, Zhaotong city, Yunnan province	*G. crassicaulis* Duthie ex Burk.	MH602366
QJ27	Tibetan Qiang autonomous prefecture of Ngawau, Sichuan	*G. dahurica* Fisch.	MH602405
QJ28	Guizhou province	*G. crassicaulis* Duthie ex Burk.	MH602367
QJ29	Yulong naxi autonomous prefecture, Lijiang city, Yunan province	*G. crassicaulis* Duthie ex Burk.	MH602368
QJ30	Heishui country, Tibetan Qiang Autonomous prefecture of Ngawau, Sichuan	*G. crassicaulis* Duthie ex Burk.	MH602369
QJ31	Heishui country, Tibetan Qiang autonomous prefecture of Ngawau, Sichuan	*G. straminea* Maxim.	MH602396
QJ32	Jingping country, Suzhou city, shanxi province	*G. dahurica* Fisch.	MH602406
QJ33	Weixi Lisu autonomous county, Diqing Tibetan autonomous Prefecture, Yunan province	*G. crassicaulis* Duthie ex Burk.	MH602370
QJ34	Keshiketeng Banner, Linxi County, Neimenggu province	*G. straminea* Maxim.	MH602397
QJ35	Nima town, Maqu country, Gannan Tibetan autonomous prefecture, Gansu province	*G. straminea* Maxim.	MH602398
QJ36	Tibetan Qiang autonomous prefecture of Ngawau, Sichuan	*G. straminea* Maxim.	MH602399
QJ37	Tibet autonomous region	*G. crassicaulis* Duthie ex Burk.	MH602371
QJ38	Ping'an country, Haidong city, Qinghai province	*G. straminea* Maxim.	MH602400
QJ39	Yunan province	*G. crassicaulis* Duthie ex Burk.	MH602372
QJ40	Yulong naxi autonomous prefecture, Lijiang city, Yunan province	*G. crassicaulis* Duthie ex Burk.	MH602373
QJ41	Dali Bai autonomous prefecture, Yunan province	*G. crassicaulis* Duthie ex Burk.	MH602374
QJ42	Tibet autonomous region	*G. crassicaulis* Duthie ex Burk.	MH602375
S0	Tu autonomous county of Huzhu, Qinghai province	*G. dahurica* Fisch.	MH602402
S1	Yunan province	*G. crassicaulis* Duthie ex Burk.	MH602377
S2	kunming city, Yunna province	*G. crassicaulis* Duthie ex Burk.	MH602378
S3	kunming city, Yunna province	*G. crassicaulis* Duthie ex Burk.	MH602379
S4	Yunan province	*G. crassicaulis* Duthie ex Burk.	MH602380

Li *et al. Chin Med*   (2020) 15:16

Page 5 of 14

Table 1 (continued)

Sample ID	Origins	Species	GenBank accession nos.
S5	Lijiang city, Yunan province	*G. crassicaulis* Duthie ex Burk.	MH602381
S6	Yunan province	*G. crassicaulis* Duthie ex Burk.	MH602382
S7	Tibetan autonomous county of Muli, Sichuan province	*G. crassicaulis* Duthie ex Burk.	MH602383
S8	Yunan province	*G. crassicaulis* Duthie ex Burk.	MH602376
S9	Yunan province	*G. macrophylla* Pall.	MH602384
S10	Unknown	*G. straminea* Maxim.	MH602401
S11	Gansu province	*G. macrophylla* Pall.	MH602385
S12	Nei Monggol autonomous region	*G. dahurica* Fisch.	MH602407
S13	Zhangjiakou city, Hebei province	*G. dahurica* Fisch.	MH602408
S14	Helongjiang province	*G. dahurica* Fisch.	MH602403
S16	Nei Monggol autonomous region	*G. dahurica* Fisch.	MH602404
S18	Gansu province	*G. macrophylla* Pall.	MH602386

QJ01–QJ42 were deposited in department of pharmacy, the first affiliated hospital of Zhengzhou University, Zhengzhou, China; S0–S18 were deposited the Institute of Chinese Materia Medica, Shanghai University of Traditional Chinese Medicine, Shanghai, China

stability. The results proved that variations of retention times were less than 0.2 min, drift values of *m/z* were less than 10 PPM, and the RSD of peak areas were all below 10% (Additional file 1: Table S1).

Raw data from Q/TOF–MS were analyzed using Markerview for peak deconvolution and peak alignment with the following parameters: initial retention time 0.5 min, final retention time 23 min, mass tolerance 10 PPM, ion intensity threshold (3000 counts) and retention time tolerance 0.1 min. The data were combined into a single matrix by aligning peaks with the same mass-retention time pair together from each data file in the data set. The ion intensities of each peak detected (2806 MS features for ESI- modes) were normalized to the sum of the peak intensities in each sample. After normalization, the data was processed according to the "80% rule", briefly only variables with values above zero presenting in at least 80% of each group were kept for the following analysis [14].

¹H-NMR profiles analysis of the collected Qinjiao

The methanol extracting supernatants (600 μL) were dried down using a centrifugal vacuum concentrator and were redissolved in 600 μL of MeOD. After mixing well, 450 μL of reconstitution wan transferred into the 5 mm NMR tubes (Norell, Landisville, NJ, USA) for NMR analysis.

NMR spectral data were obtained at 300 K on a Bruker 600-MHz AVANCE III NMR spectrometer (Bruker, Germany), equipped with a 5.0-mm BBO probe, operating at 600.13 MHz for ¹H. The zg30 Bruker pulse program was used for 1D ¹H NMR, with a TD of 64 k, relaxation delay of 1 s, spectral width of 20 ppm,

and 256 scans. A line-broadening factor of 0.3 Hz was applied to FIDs before Fourier transformation. All NMR spectra were phased and baseline-corrected manually using TOPSPIN 3.5 (Bruker, Germany). The spectra were referenced internally to the chemical shift of H-3 signal of gentiopicroside at 7.46 ppm. Each ¹H-NMR spectrum over the ranged 0.5–10.0 ppm was reduced to 238 regions of equal width (0.04 ppm) and the signal intensity in each region was integrated using AMIX (version 3.9, Bruker, Germany). The region of 4.75–5.20 ppm was removed prior to any statistical analysis in order to eliminate any residual water signal. Then data was normalized in AMIX by dividing each integrated segment by the total area of the spectrum to reduce any significant.

Statistical analysis and compound annotation

Output data from TOF–MS or NMR analysis was separately imported into SIMCA (version 14.0, Umetrics, Umeå, Sweden) for multivariate statistical analysis (MS data unit variance scaled, NMR data pareto-scaled). To provide comparative interpretations and visualization of the metabolic differences among the four species of Qinjiao, PCA and OPLS-DA were applied to the TOF–MS or NMR data set. The quality of the models was described by R2X and Q2 values. R2X shows the proportion of variance in the data explained by the models and indicates goodness of fit. The value closer to 1 indicates the goodness of fit. Q2, on the other hand, shows the proportion of variance in the data predictable by the model and indicates predictability. The results were visualized in the form of score plots, where each point represents an individual sample (to

Li *et al. Chin Med*   (2020) 15:16

Page 6 of 14

show the group clusters), and loading plots or S-plots, where each coordinate represents one mass-retention feature or ^{1}H-NMR spectral region (to identify the variables contributing to the classification). The variable importance of projection (VIP) is the vector to summarize the total importance of the variable in explaining the model. The corresponding variables with VIP > 1.0 were chosen as potential discriminative metabolites. To justify the OPLS-DS models, analysis of variance testing of Cross-Validated predictive residuals (CV-ANOVA) were conducted. CV-ANOVA is a diagnostic tool for assessing the reliability of PLS and OPLS models. The *P* value produced by CV-ANOVA indicates the probability level. The common practice is to interpret a p-value lower than 0.05 as pointing to a significant model. Statistical analysis was also performed using one-way analysis of variance (ANOVA) followed by Tukey's multiple comparison test (SPSS, Chicago, IL, USA). A probability of P < 0.05 was considered to be statistically significant between two groups.

LC–MS Peaks were identified according to actual mass, MS/MS fragments and retention time (RT). First, the m/z value of the molecular ion of interest was searched against a self-build Qinjiao constituent Database, where data was collected from published researches [15, 16]. Then, the putative identifications were verified by comparing the MS2 fragmentations. Part of the constituents were further identified by reference standards. ^{1}H-NMR signals were assigned by comparing the spectrum of Qinjiao with that of gentiopicroside, loganic acid, sweroside, swertiamarin or sucrose by Chenomx NMR suit (version7.6, Chenomx, Edmonton, Canada) with method described in our previous work [17].

Results

ITS2 comparation

ITS2 sequences from collected Qinjiao samples were submitted to GenBank database (Accession numbers were listed in Table 1), assembled with CodonCode Aligner 3.7.1 (CodonCode Co., Dedham, MA, USA)

and aligned using ClustalW. Kimura 2-Parameter (K2P) distances. GC content of base and NJ trees were calculated and constructed using the MEGA X software with the Bootstrap method (500 resampling) and K2P model [18]. The distances within or among species are separately list in Table 2. The average ITS2 region was 497 bp in length in 4 species of Qinjiao, and the G+C content ranged from 55.7% to 56.2%, with an average of 56.0% (Table 2). A neighbor-joining (NJ) tree of ITS2 barcode was formed on the basis of K2P model (Fig. 2).

TOF–MS data metabolomics

Representative base peak intensity (BPI) chromatograms of *G. crassicaulis* is shown in Fig. 3. By comparing actual mass, MS/MS fragments and retention time (RT) of target compounds, 28 constituents were identified, among which 17 were further identified by reference standards. The compound information is list in Table 3, with XIC chromatography shown in Additional file 2: Fig. S1. ANOVA followed by Tukey's multiple comparison test were conducted for these 28 compounds (partly shown in Fig. 4).

Multivariate analysis of the TOF–MS data was carried out. Initially, unsupervised PCA-X analysis were conducted among groups, showing preferably discriminative distribution (not shown, R2X = 0.661, Q2 = 0.398). Subsequently, to maximize the variation among groups and to determine the variables that contributed to this variation, supervised OPLS-DA model (Fig. 5a) was employed among four species of Qinjiao, with R2X = 0.38, R2Y = 0.666, Q2 = 0.549. The loading plot (Fig. 5b) revealed the correlations between class (species) and variables (MASS feature), where variables clustering close to each class were considered to make great contributions to the classification. Furthermore, it was noticed that *G. crassicaulis* and *G. dahurica* clustered furthest from each other in the score plot (Fig. 5a). To explore the difference, OPLS-DA analysis for these two groups was conducted, with R2Y 0.924 and Q2 0.864 (Fig. 5c). Corresponding S-plot (Fig. 5d) was analyzed, which was commonly used and effectively showed the difference between groups. Part of the variable selected from S-plot

Table 2 Sequence sizes, percent G+C content and mean distance intra/inter each spices of collected Qinjiao samples

Species	ITS2 length (bp)	G+C content (%)	Mean distance intra species	Mean distance inter species		
				1	2	3
1 *G. crassicaulis* Duthie ex Burk.	495.8	56.0	0.0274			
2 *G. dahurica* Fisch.	496.0	55.9	0.0229	0.0371		
3 *G. macrophylla* Pall.	498.2	55.7	0.0062	0.0312	0.0246	
4 *G. straminea* Maxim.	498.8	56.2	0.0130	0.0288	0.0220	0.0146

Li *et al. Chin Med*   (2020) 15:16

Page 7 of 14
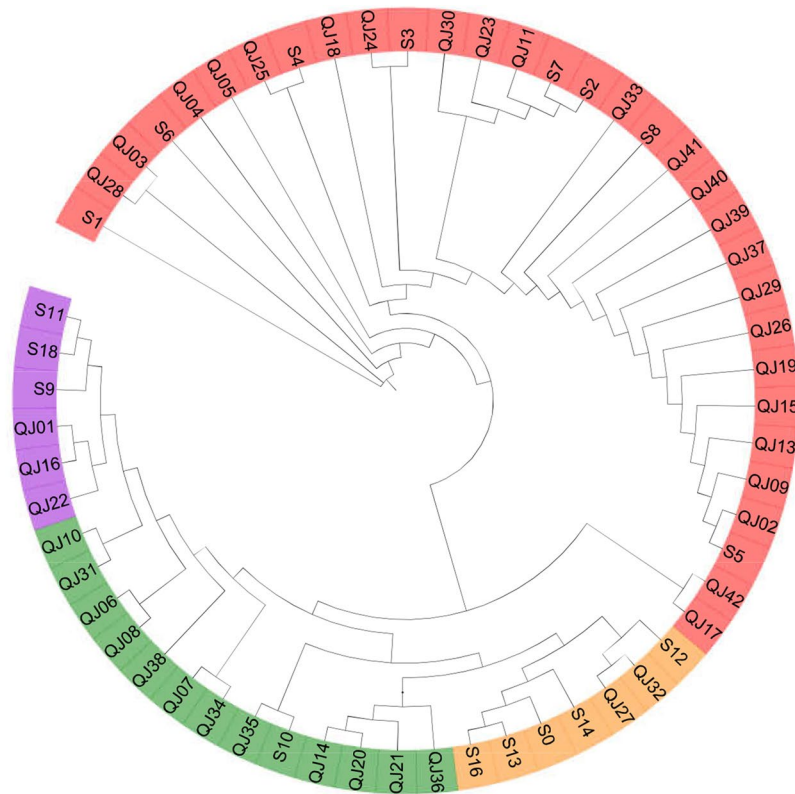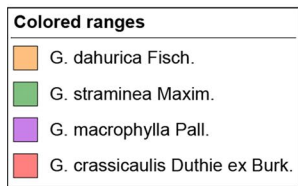
Fig. 2 NJ tree of *G. macrophµlla*, *G. straminea*, *G. crassicaulis* and *G. dahurica*
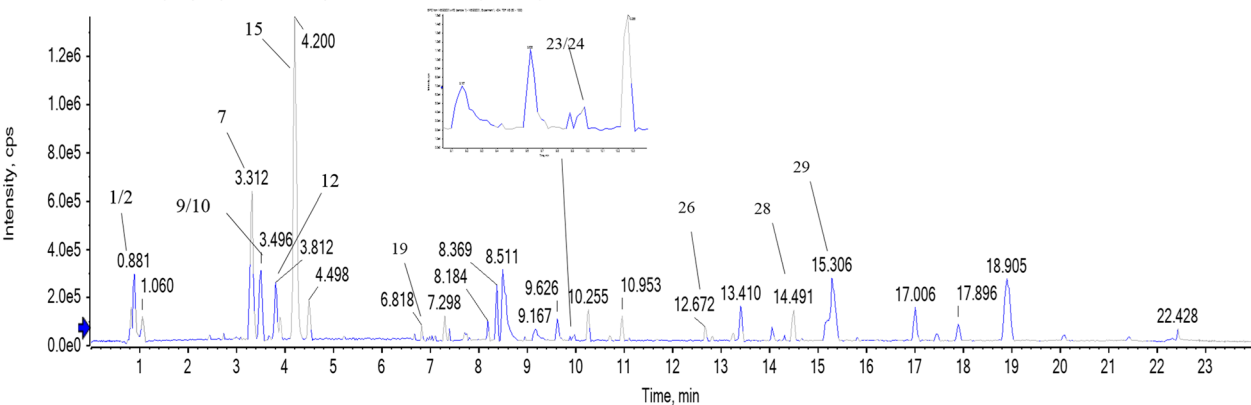

Fig. 3 Representative BPI chromatograms of *G. crassicaulis*, with part of the constituents identified. Note: 1. Sucrose, 2. Swertiajaposide A, 7. Loganic acid, 9. 6′-*O*-β-ᴅ-Glucosylgentiopicroside, 10. Qinjiaoside A, 12. Swertiamarin, 15. Gentimacroside, 19.Vitexin, 23. Ursolic Acid, 24. Oleanolic acid, 26. 2α-hydroxyl ursolic acid, 28. β-sitosterone, 29. Roburic acid

with VIP value > 1.0 and their abundances were shown in Additional file 3: Table S2. The established OPLS-DA models were further validated by CV-ANOVA test, with P valve less than 0.05 indicating significant models (Additional file 4: Table S3).

¹H-NMR data metabolomics

A representative 1D ¹H-NMR spectrum of G. *crassicaulis* is shown in Fig. 6. Signal assignments were list in Table 4. Fore iridoids, gentiopiciroside, swertiamarin, loganic acid, and sweroside were identified ultimately by

Table 3 Characterization of chemical constituents in Qinjiao by UHPLC-QTOF–MS in ESI-mode

No.	tR/min	Observed mass	Molecular weight	Molecular formula	MS/MS fragments ions (m/z)	Identified compound
1[a]	0.87	341.1086	342.1161	$C_{12}H_{22}O_{11}$	179.0562, 161.0459, 131.0351, 119.0350, 89.0241, 59.0135	Sucrose
2[b]	0.88	387.1148	388.1369	$C_{17}H_{24}O_{10}$	341.1090, 195.0507, 179.0562, 59.0238, 59.0136	Swertiajaposide A
3[*]	1.63	191.0196	192.0270	$C_6H_8O_7$	111.0086, 87.0087, 67.0188, 57.0345	Citric acid
4[b]	2.56	169.0870	170.0943	$C_9H_{14}O_3$	123.0806, 121.0663, 110.9975, 95.0503, 67.0559, 61.9881	Isoboonein
5[b]	2.73	315.0719	316.0794	$C_{13}H_{16}O_9$	315.0723, 153.0181, 109.0293	5-(β-D-Glucopyranosyl)-2-hydroxybenzoic acid
6[b]	2.99	537.1828	538.1897	$C_{22}H_{34}O_{15}$	375.1297, 221.0264, 213.0769, 169.0869, 113.0241, 179.0557, 89.0242, 69.0344	Loganic acid 11-*O*-β-glucopyranosylester
7[a]	3.31	399.1258,	376.1369	$C_{16}H_{24}O_{10}$	213.0766, 169.0868, 151.0761, 119.3047, 113.0240, 89.0241, 69.0342, 59.0135	Loganic acid
8[a]	3.39	451.1446	406.1475	$C_{17}H_{26}O_{11}$	405.1165, 243.0872, 141.0553, 101.0242, 89.0241, 59.0135	Morroniside
9[a]	3.42	563.1620	518.1635	$C_{22}H_{30}O_{14}$	221.0659, 179.0552, 161.0449, 119.0343, 89.0237	6′-*O*-β-D-Glucosylgentiopicroside
10[b]	4.49	403.1245	404.1319	$C_{17}H_{24}O_{11}$	151.0764, 125.0242, 113.0243, 89.0243, 59.0137	Qinjiaoside A
11[b]	3.67	519.1726	520.1791	$C_{22}H_{32}O_{14}$	519.1743, 323.0995, 213.0767, 151.0762, 125.0244, 59.0142	Swertiapunimarin;6′-*O*-Glucopyranosylsweroside
12[a]	3.73	419.1193	374.1212	$C_{16}H_{22}O_{10}$	149.0605, 141.0188, 119.0347, 89.0238	Swertiamarin
13[b]	3.89	389.1085	390.1161	$C_{16}H_{22}O_{11}$	183.0660, 165.0557, 121.0655, 89.0241, 69.0343	Secologanoside
14[a]	4.11	401.1074	356.1107	$C_{16}H_{20}O_9$	149.0604, 119.0347, 89.0239, 71.0136, 59.0133	Gentiopicorside
15[b]	4.17	531.1529	532.1581	$C_{26}H_{28}O_{12}$	235.0612, 191.0714, 173.0608, 163.0767, 149.0606, 89.0243	Gentimacroside
16[a]	4.4	403.1244	358.1263	$C_{16}H_{22}O_9$	357.1193, 195.0666, 179.0564, 125.0241, 119.0347, 151.0763, 89.0242, 81.0343, 59.0136 9	Sweroside
17[a]	5.78	447.0936	448.1005	$C_{21}H_{20}O_{11}$	429.1045, 369.0630, 357.0616, 327.0508, 297.0398, 285.0404, 61.9884	Isoorientin
18[a]	6.62	431.0983	432.1056	$C_{21}H_{20}O_{10}$	341.0668, 323.0563, 311.0559, 283.0608, 281.0451	Isovitexin
19[b]	6.76	477.1032	432.1056	$C_{21}H_{20}O_{10}$	431.0983, 323.0766, 315.0720, 161.0238, 153.0187, 152.0048	Vitexin
20[b]	7.04	875.2236	876.2324	$C_{40}H_{44}O_{22}$	875.2251, 833.2133, 739.2096, 713.1740, 577.1562, 535.1466, 315.0723, 153.0191,	Macrophylloside A
21[a]	7.08	301.0345	302.0426	$C_{15}H_{10}O_7$	193.0142, 149.0248, 121.0312	Quercetin
22[a]	7.19	285.0397	286.0477	$C_{15}H_{10}O_6$	192.0061, 177.0194, 142.9487, 119.0135, 87.0237	Kaempferol
23[a]	9.89	455.3531	456.3604	$C_{30}H_{48}O_3$	409.2535, 152.9962	Ursolic acid
24[a]	9.92	455.3529	456.3604	$C_{30}H_{48}O_3$	409.2535, 152.9962	Oleanolic acid
25[b]	10.73	255.2308	256.2402	$C_{16}H_{32}O_2$	255.2326, 237.2210	Plamitic acid
26[a]	13.5	621.4381	576.4390	$C_{35}H_{60}O_6$	575.4681, 303.8955, 295.2278, 191.9469, 89.0241	Daucosterol
27[a]	14.5	457.3658	414.3862	$C_{29}H_{50}O$	457.3671, 411.3623	β-Sitosterone
28[a]	15.3	439.3581	440.3654	$C_{30}H_{48}O_2$	439.3565, 421.3469	Roburic acid

Li *et al. Chin Med* (2020) 15:16

Page 9 of 14

Table 3 (continued)

a Identified by comparing with the reference standards

b Putative identifications by MS and MS2 fragmentations

Chenomx NMR suit (version7.6, Chenomx, Edmonton, Canada).

NMR data acquired was also analyzed by PCA-X model (R2X = 0.943, Q2 = 0.817) and OPLS-DA models (R2X = 0.38, R2Y = 0.666, Q2 = 0.549). As shown in Fig. 7a, b, samples from species of *G. crassicaulis*, *G. straminea*, *G. macrophylla*, and *G. dahurica* distributed regionally in the score plot, with the latter 3 species gradually deviating far away from the first one.

To explore the diversity between *G. crassicaulis* and *G. dahurica*, OPLS-DA analysis was achieved between them, with R2X 0.726, R2Y 0.884 and Q2 0.848 (Fig. 7c). Corresponding S plot (Fig. 7d) was generated. The established OPLS-DA models were further validated by CV-ANOVA test, with P valve less than 0.05 indicating significant models (Additional file 4: Table S3).

Discussion

ITS2 data analysis

Minimum distance within species was observed between *G. macrophylla*_and *G. straminea*, with K2P distance value 0.0146. While maximum K2P distance within species was present between *G. crassicaulis* and *G. dahurica*, with value 0.0371. The minimum interspecific distance of ITS2 region was higher than the maximum intraspecific distance, indicating that the ITS2 barcode performed well in the discrimination of four species of Qinjiao. The distances among species revealed were in accordance with discrepancy detected by following metabolomics analysis. It was illustrated that species of *G. macrophylla*, *G. straminea*, *G. dahurica* and *G. crassicaulis* can be clearly distinguished by the NJ tree. ITS2 analysis confirmed the potential discrepancy among species and guaranteed reliability of subsequent metabolomics-based species evaluation.

TOF–MS data analysis

The score plots (Fig. 5a) shows that samples from species of *G. macrophylla*, *G. straminea*, *G. dahurica* and *G. crassicaulis* located different areas in score plot, inferring distinctive chemical profiles of four species of Qinjiao. In general, *G. crassicaulis* and *G. straminea* were closest in the score plot, while *G. macrophylla* and *G. dahurica* were progressively far away from them. Maximum spatial distance was present between *G. dahurica* and *G. crassicaulis*. The result was consistent with discrepancy revealed by ITS2 analysis. The loading plot (Fig. 5b) revealed MASS features making

great contributions to the classification, which was further confirmed by ANOVA test. Flavonoids (isovitexin, morronside, quercetin) and triterpenoids (oleanolic acid, ursolic acid, roburic acid, β-sitosterone, daucosterol), as well as certain iridoids (macrophylloside A and Qinjiaoside A) were significant higher in *G. dahurica*. than other 3 species; while other(seco)iridoids (swertiamarin, secologanoside, loganic acid, gentimacroside, loganic acid 11-*O*-β-glucopyranosylester) and citric aicd were richer in other 3 species of Qinjiao than *G. daurica*. No obvious distinction was detected in contents of sweroside, sucrose, swertiapunimarin, and swertiajaposide A among four species of Qinjiao.

OPLS-DA score plot (Fig. 5c) and corresponding S-plot (Fig. 5d) of *G. crassicaulis* and *G. dahurica* confirmed maximum K2P distance revealed by ITS2 analysis. It was noticed that MASS features of 401.1074_4.19 (gentiopicroside), 375.1276_3.29 (loganic aicd), 419.1193_3.81(swertiamarin), 191.0200_1.09(citric acid), 563.1601_3.50(6′-*O*-β-D-glucosyl-gentiopicroside), and 389.1087_3.89 (secologanic acid) were richer in *G. crassicaulis*, while MASS features of 439.3562_15.30 (roburic aicd), 455.3510_9.93 (ursolic Acid), 455.3505_9.99 (oleanolic acid), 457.3658_14.5(β-sitosterone) and 451.1456_3.40 (morroniside) were richer in *G. dahurica*. The discrepancy was consistent with ANOVA test result (Fig. 4). It seems that (seco)iridoids like loganic acid, gentiopicroside or swertiamarin were richer in specie of *G. crassicaulis*, while flavonoid (morroniside) and triterpenoids (roburic aicd, ursolic acid, oleanolic acid, β-sitosterone) were richer in specie of *G. dahurica*. The discrepancy was consistent with previous reports [19, 20], which reported higher contents of gentiopicroside, loganic acid, sertiamarin, and 6′-*O*-β-D-glucosyl-gentiopicroside in *G. crassicaulis* comparing with *G. dahurica*.

¹H-NMR data analysis

According to the score plot (Fig. 7a, c), NMR based metabolomics validated results revealed by MS based metabolomics. The S-plot (Fig. 7d) between these two groups showed that signal abundance from 3 to 7 ppm was richer in *G. crassicaulis*, while which from around 0.8–2 ppm was richer in *G. dahurica*. Unfortunately, limited to the complexity of the ¹H-NMR spectra, compounds related to the abundance difference were not directly identified. However, the difference
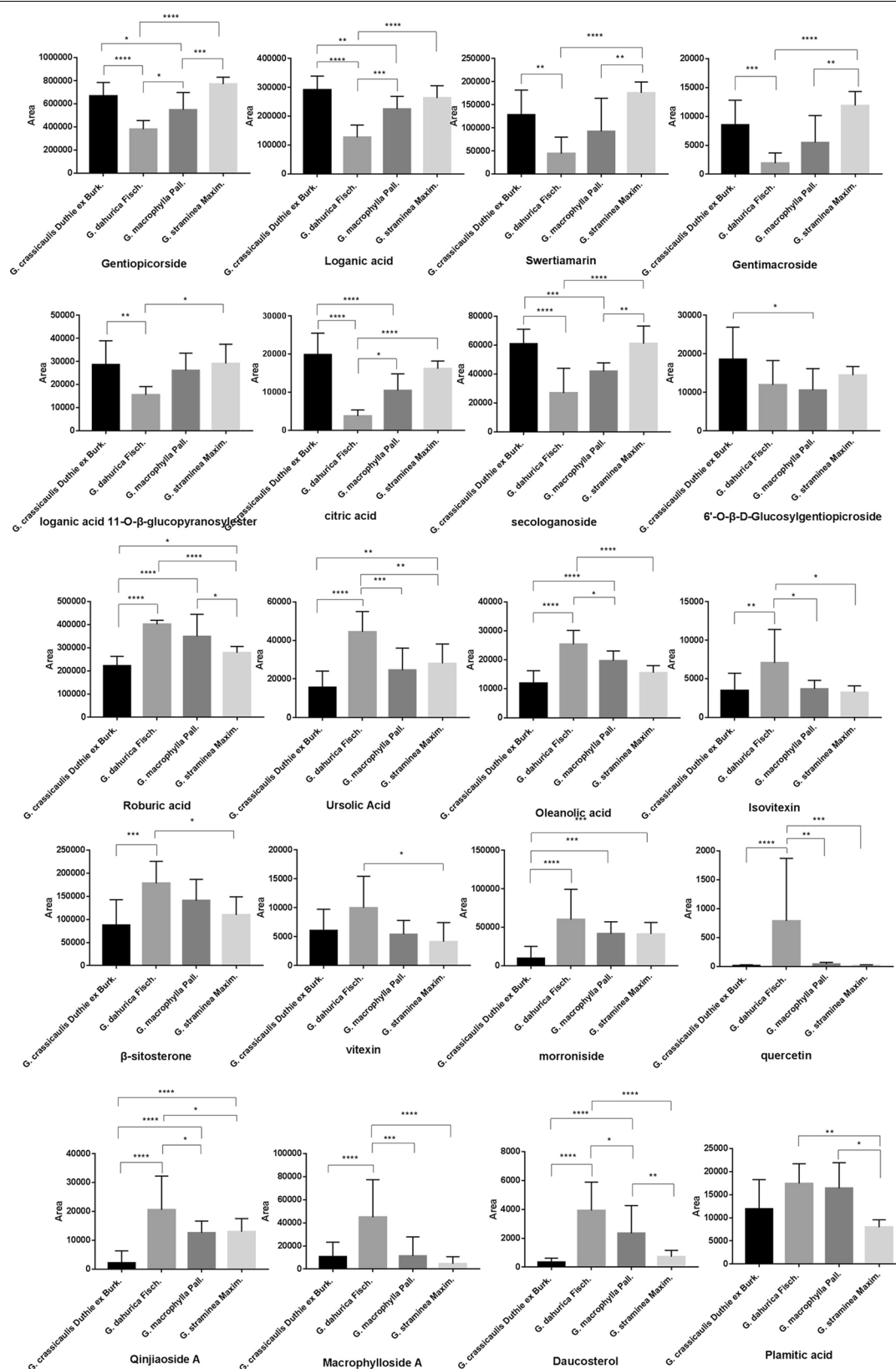
Li *et al. Chin Med*   (2020) 15:16

Page 10 of 14

Fig. 4 Part of ANOVA test result of identified constituents by TOF–MS. *P < 0.05; **P < 0.01; ***P < 0.001;****P < 0.0001
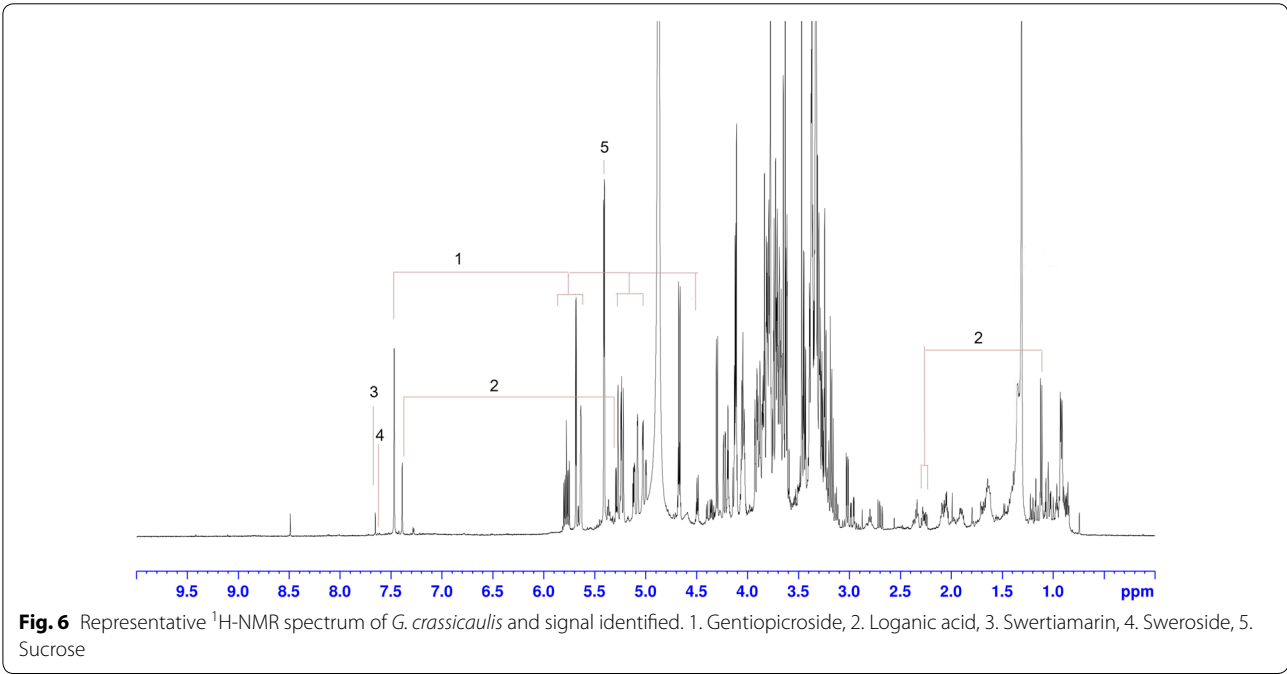
Li *et al. Chin Med* (2020) 15:16

Page 11 of 14

Fig. 5 Score plot and loading plot of TOF–MS data. **a** Score plot of 4 species of Qinjiao; **b** loading plot of OPLS-DA model; **c** OPLS-DA score plot of *G. crassicaulis* and *G. dahurica* species; **d** S-plot of *G. crassicaulis* and *G. dahurica* species

Fig. 6 Representative ^{1}H-NMR spectrum of *G. crassicaulis* and signal identified. 1. Gentiopicroside, 2. Loganic acid, 3. Swertiamarin, 4. Sweroside, 5. Sucrose

Li *et al. Chin Med*   (2020) 15:16

Page 12 of 14

Table 4 Characteristics of ¹H-NMR signals observed in Qinjiao extract

Compound	Group	Chemical shift δ (ppm)
Gentiopicroside	3-H(d)	7.47
	8-H(m)	5.76
	1-H(d)	5.66
	6-H(m)	5.63
	10-CH$_2$(dt)	5.22
	7=CH(m)	5.00–5.10
	1-glc-1′(d) –CH (anomeric)	4.67
Loganic acid	3-H(d)	7.38
	1-H(d)	5.28
	5-H(m)	2.24
	9-H(m)	1.98
	8-H(d)	1.10
	1-glc-1′(d) –CH (anomeric)	4.66
Swertiamarin	3-H(s)	7.65
	9-H(d)	2.93
Sweroside	3-H(d)	7.60
Sucrose	–CH (anomeric)(d)	5.40

a Letters in parentheses indicate the peak multiplicity property of proton NMR signal

s singlet, *d* doublet, *dd* double doublet, *dt* double triplet, *t* triplet, *m* multiplet, *br* broad

was confirmed and can be explained by preceding MS based metabolomics. The signal intensity discrepancy present in ¹H-NMR spectra coincided with abundance discrepancy MS revealed (Fig. 5d). Richer abundance of triterpenoids in *G. dahurica* produced richer signal intensity in characteristic region range of 0.5 to 2.4 ppm (signal from Skeleton proton) and 3.24 to 3.28 ppm(H-3) [21]. On the other side, higher concentration of (seco)iridoids produced higher signal intensity of 2.4 to 5 ppm (signal from (seco)iridoids skeleton proton) and 7.0–7.4 ppm(signal of H-3) [22]. The consistence by NMR and TOF−MS metabolomics confirmed the chemical discrepancy between *G. crassicaulis* and *G. dahurica*. The discrepancy may be helpful for distinguishing of these two species and may lead to potential pharmacodynamics discrepancy, which remains to be investigated.
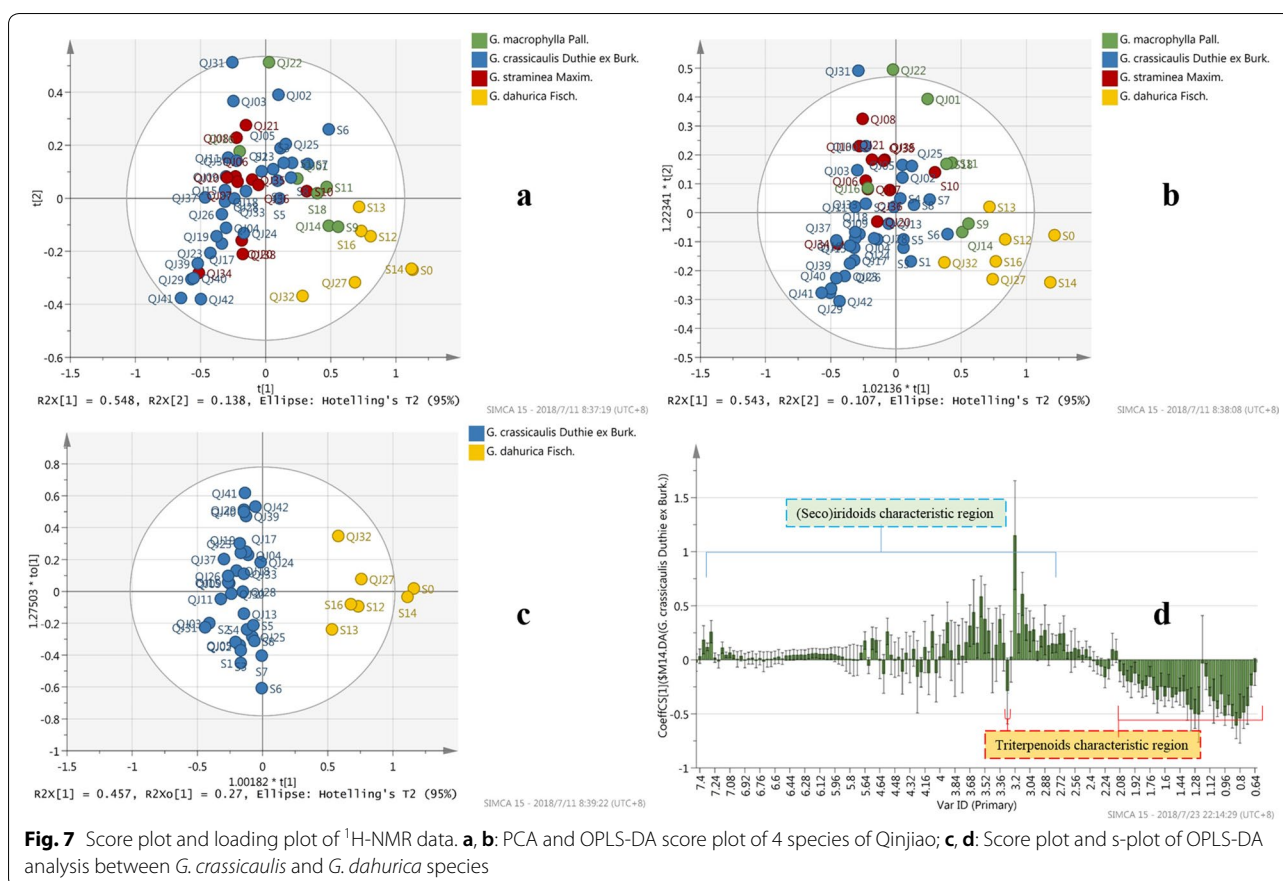
ITS2, TOF−MS and NMR integration

ITS2 based gene comparison can present species distance or genetic relationship among species. Currently, ITS2 is the mostly commonly used region for the barcoding and authentication of herbal medicinal materials. In future, species authentication by ITS2 sequence (or other genetic method) may be precondition of quality evaluation of MSRHM. However, environmental implication and chemical discrepancy were not reflected. Information of quality and origin shall ultimately rely on chemical method. On the other side, TOF−MS or NMR based metabolomics analysis providing systemic chemical information among species, and can be powerful tool for quality investigations. TOF−MS bears the advantage of high sensitivity, high specificity, and thus offers maximum amount of information for quality control. However, TOF−MS based platform suffers from the disadvantage of inhomogeneous ionization propensities and time-consuming samples preparation procedures. In contrast, NMR platform possesses disadvantages of lower sensitivity and limited specificity, as well as advantages of homogenous signal response and simple sample preparations [23]. In general, a combination of ITS2 sequence comparations and TOF−MS as well as NMR based metabolomics analysis can validated each other and provided more comprehensive quality investigation for MSRHM [24].

Conclusion

In this study, a new integrated quality evaluation strategy was proposed for MSRHM of Qinjiao employing ITS2 sequence comparation, TOF−MS and NMR based metabolomics analysis. At first, gene comparison based on ITS2 sequence was conducted among 4 species of Qinijao. Then, TOF−MS and NMR based metabolic analysis were applied to investigate species discrepancy among four species of Qinjiao. It turned out that species discrepancy revealed among species were consistent by ITS2 sequencing, NMR and TOF−MS based metabolomics. Maximum species difference was noticed between *G. crassicaulis* and *G. dahurica*. Chemical difference among species based on TOF−MS and NMR were tentative explored. For TOF−MS profiling of Qinjiao, 28 constituents were tentative identified, 17 of which were further confirmed by standards. For ¹H-NMR spectra of Qinjiao, signals from 5 compounds were assigned. Contents discrepancies were investigated by ANOVA analysis. It turned out that MS based metabolomics coincided with NMR based metabolomics result, and explained the intensity discrepancy in ¹H-NMR spectra.

The current research demonstrates that integration of ITS2 sequence comparation and UPLC/Q-TOF MS as well as ¹H-NMR based metabolomics analysis can be a powerful strategy for quality investigation of MSRHM.

Li *et al. Chin Med*   (2020) 15:16

Page 13 of 14

Fig. 7 Score plot and loading plot of ^{1}H-NMR data. **a**, **b**: PCA and OPLS-DA score plot of 4 species of Qinjiao; **c**, **d**: Score plot and s-plot of OPLS-DA analysis between *G. crassicaulis* and *G. dahurica* species

Supplementary information

Supplementary information accompanies this paper at https://doi.org/10.1186/s13020-020-0292-3.

Additional file 1: Table S1. Drift of retention times, *m/z* and the RSD of peak areas of 5 selected characteristic features from QC samples during the analysis.

Additional file 2: Fig. S1. XIC chromatography of 28 identified constituents.

Additional file 3: Table S2. Part of the variable with VIP value > 1.0 from OPLS-DA analysis of *G. crassicaulis* and *G. dahurica*.

Additional file 4: TAble S3. P value of CV-ANOVA for OPLS-DA models based on MS or NMR analysis.

Abbreviations
MSRHM: multi-species resourced herb medicine; *G. macrophylla*: *Gentiana macrophylla* Pall; *G. straminea*: *Gentiana straminea* Maxim; *G. crasicaulis*: *Gentiana crassicaulis* Duthie ex Burk; *G. daurica*: *Gentiana dahurica* Fisch; ITS2: internal transcribed spacer 2; UPLC-Q-TOF–MS: ultra performance liquid chromatography quadrupole time-of-flight mass spectrometry; ^{1}H-NMR: proton nuclear magnetic resonance spectrometer; PCA: principal component analysis; OPLS-DA: orthogonal partial least squares discrimination analysis; ANOVA: one-way analysis of variance; VIP: variable importance in the projection value.

Authors' contributions
All persons who meet authorship criteria are listed as authors, and all authors certify that they have participated sufficiently in the work to take public responsibility for the content, including participation in the concept, design, analysis, writing, or revision of the manuscript. Furthermore, each author certifies that this material or similar material has not been and will not be submitted to or published in any other publication. The specific contributions made by each author have been listed as follows: Zeyun Li: conception and design of study, acquisition of data and drafting the manuscript; Yue Du, Yongliang Yuan: acquisition of data, analysis and interpretation of data; Xiaojian Zhang, Xin Tian: revising the manuscript critically for important intellectual content; Zhengtao Wang: conception and design of study, analysis and interpretation of data. All authors read and approved the final manuscript.

Availability of data and materials
The datasets used and/or analyzed during the current study are available from the corresponding author on reasonable request.

Ethics approval and consent to participate
Not applicable.

Consent for publication
Not applicable.

Li *et al. Chin Med*   (2020) 15:16

Page 14 of 14

References

1. Wang Y, Lou Z. Study of Radix Gentianae Macrophyllae. Chin Pharm J. 1987;22:153–9.
2. Nie A, Lin Z, Wang Y, Zhang B. Study on chemical constituents and pharmacological action of gentiana gentiana macrophylla. Chin Trad Herb Drugs. 2017;48:597–608.
3. China Pharmacopoeia National Pharmacopoeia Committee, Beijing.
4. Wagner H, Bauer R, Melchart D, Xiao PG, Staudinger A. Chromatographic fingerprint analysis of herbal medicines Volume III. 中草药(英文版). 2011. pp. 137–46.
5. Shi D, Zhang J, Sun L. Necessity of the research on equal quantity based on the quality investigation of three multi-origin pieces. China J Trad Chin Med Pharm. 2018;33:320–4.
6. Cao X, Wang Z. Simultaneous determination of four iridoid and secoiridoid glycosides and comparative analysis of Radix Gentianae Macrophyllae and their related substitutes by HPLC. Phytochem Anal. 2010;21:348–54.
7. Qi S, Shang P, Zhang Y, Jia N, Jiao H, Zhao W, et al. HPLC fingerprint and LC-TOF-MS analysis on extract from roots of Gentiana macrophylla. Chin Herbal Med. 2012;04:245–51.
8. Wang Y, Ahmad B, Duan B, Zeng R, Huang L. Chemical and genetic comparative analysis of Gentiana crassicaulis and Gentiana macrophylla. Chem Biodivers. 2016;13:776–81.
9. Michel CI, Meyer RS, Taveras Y, Molina J. The nuclear internal transcribed spacer (ITS2) as a practical plant DNA barcode for herbal medicines. J Appl Res Med Arom Plants. 2016;3:94–100.
10. Luo Y, Ma P, Yao H, Xin T, Hu Y, Zheng S, et al. Identification of Gentianae Macrophyllae Radix using the ITS2 barcodes. Acta Pharmaceutica Sinica. 2012;47:1710–7.
11. Freitas J, Alves EF, Silva L, Zocolo GJ, De EB, Gramosa N. Chemometric analysis of NMR and GC datasets for chemotype characterization of essential oils from different species of Ocimum. Talanta. 2018;180:329.
12. Chen S, Yao H, Han J, Xin T, Pang X, Shi L, et al. Principles for molecular identification of traditional Chinese materia medica using DNA barcoding. China J Chin Materia Med. 2013;38:141–8.
13. Luo K, Chen SL, Chen KL, Song JY, Yao H, Ma XY, et al. Assessment of candidate plant DNA barcodes using the Rutaceae family. Sci China Life Sci. 2010;53:701–8.
14. Rubingh CM, Bijlsma S, Derks EPPA, Bobeldijk I, Verheij ER, Kochhar S, et al. Assessing the performance of statistical validation tools for megavariate metabolomics data. Metabolomics. 2006;2:53–61.
15. Zhang X, Zhan G, Jin M, Zhang H, Dang J, Zhang Y, et al. Botany, traditional use, phytochemistry, pharmacology, quality control, and authentication of Radix Gentianae Macrophyllae—a traditional medicine: a review. Phytomedicine. 2018;46:142–63.
16. Wang C, Dong H, Bao Y, Chen X, Hai Y, Zeng R. Rapid analysis on chemical constituents from roots of Gentiana crasicaulis by ultra-high performance liquid chromatography coupled with hybrid quadrupole-orbitrap mass spectrometry. Chin Trad Herbal Drugs. 2016;47:3175–80.
17. Yang X, Zhang K, Li Z, Wang Z. Targeted profiling qHNM for determination of Gentiopicroside and loganic acid in 4 species of Gentianae Macrophyllae Radix. Chin J Exp Trad Med Formulae. 2017;23:98–103.
18. Tamura K, Stecher G, Peterson D, Filipski A, Kumar S. MEGA6: molecular evolutionary genetics analysis version 6.0. Mol Biol Evol. 2013;30:2725–9.
19. Yang Y, Ma X, Lu Y, Lv P, Lin L, Wang Z, et al. Contents of seven indicative constituents in seven kinds of Gentiana macrophylla by UPLC. Chin Trad Herb Drugs. 2016;47:1968–73.
20. Cao X, Wang Z, Wang Z. Comparative analysis of contents of four iridoid glucosides in different organs of four species of Gentiana L. J Plant Resourc Environ. 2012;21:58–63.
21. Li Z, Welbeck E, Yang L, He C, Hu H, Song M, et al. A quantitative (1)H nuclear magnetic resonance (qHNMR) method for assessing the purity of iridoids and secoiridoids. Fitoterapia. 2015;100:187–94.
22. Li Z, Welbeck E, Wang R, Liu Q, Yang Y, Chou G, et al. A universal quantitative ¹H nuclear magnetic resonance (qNMR) method for assessing the purity of dammarane-type ginsenosides. Phytochem Anal. 2015;26:8–14.
23. Pan Z, Raftery D. Comparing and combining NMR spectroscopy and mass spectrometry in metabolomics. Anal Bioanal Chem. 2007;387:525–7.
24. Dieterle F, Riefke B, Schlotterbeck G, Ross A, Senn H, Amberg A. NMR and MS methods for metabonomics. Methods Mol Biol. 2011;691:385–415.

Publisher's Note
Springer Nature remains neutral with regard to jurisdictional claims in published maps and institutional affiliations.